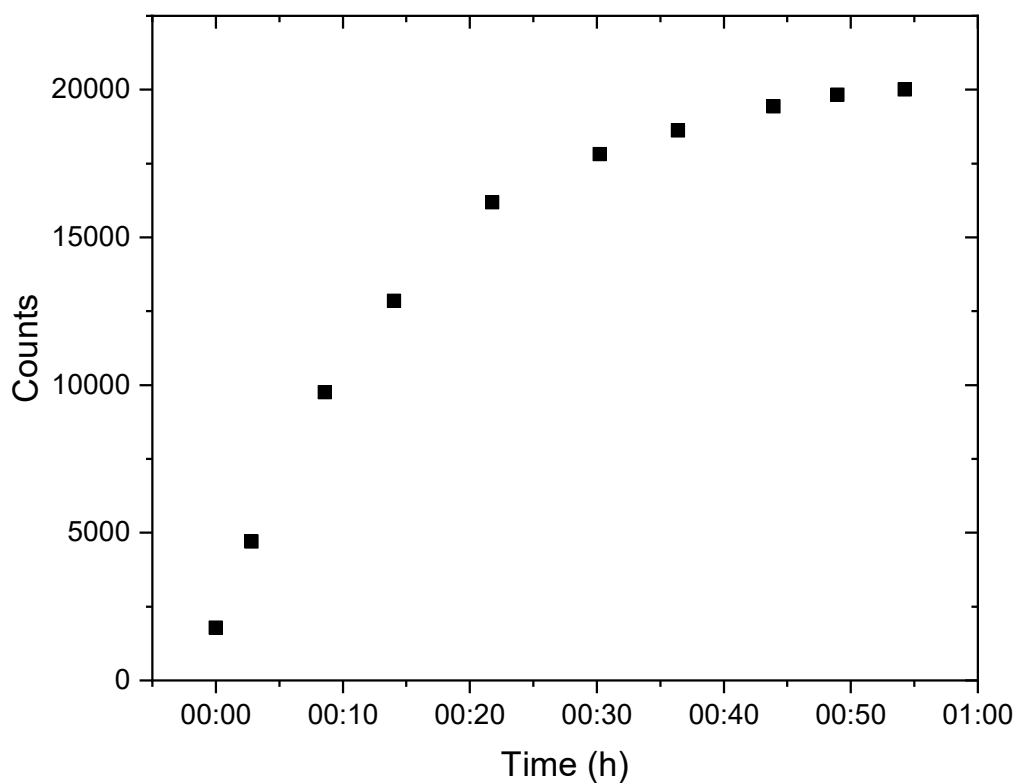


## 1 Supplementary Information

### 1.1 OPDA and DHA Reaction Time

The reaction kinetics of the condensation reaction between OPDA and DHA to form DFQ was determined. DHA and OPDA were mixed in a vial at concentrations used in the OOPAAI and every 5 min an aliquot was measured with the same setup that was used for all offline measurements. Campbell et al., 2019 (Campbell et al., 2019) and Vislisel et al., 2007 (Vislisel et al., 2007) assumed pseudo first-order kinetics for this reaction and estimated that using conditions of the OOPAAI, the reaction should be completed within minutes. However, the experiments conducted in this study (Figure S1) showed that the reaction is much slower and that it takes about 10min for 50% DHA to react. This agrees with the kinetics described in Deutsch and Weeks 1965 (Deutsch and Weeks, 1965). In the actual design of the OOPAAI a short reaction time was chosen (around 3 min) to minimize potential artefact that could occurs due to the lower pH of the DHA-OPDA condensation reaction (see main text).



**Figure S1 Formation kinetics of DFQ from the condensation reaction of DHA with OPDA.**

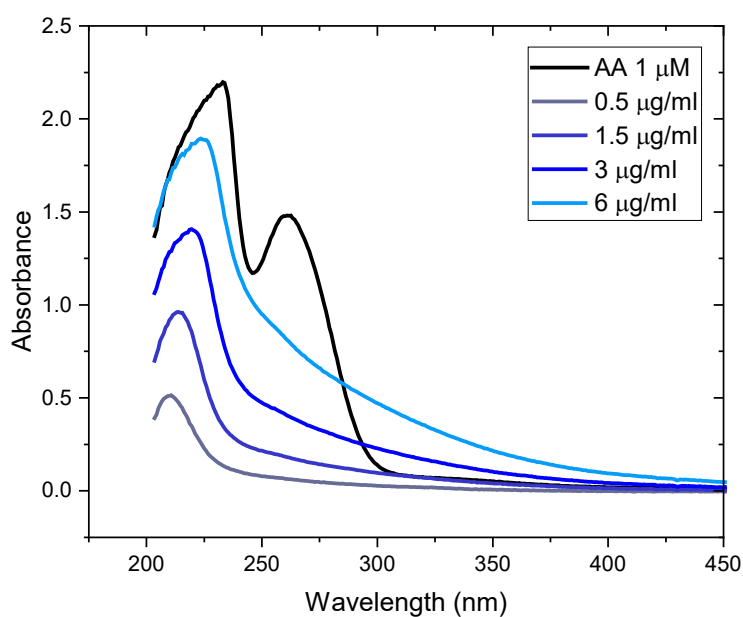
## 15 1.2 Absorbance AA and Filter Extract

For offline measurements of OP with AA, the AA decay is mostly quantified with UV absorbance measurements and not via fluorescence detection (Fang et al., 2015; Perrone et al., 2019; Zhang et al., 2021). We performed some preliminary tests to evaluate if absorption measurement would also be a suitable analysis strategy for an online AA instrument. The potentially biggest issue for an absorbance-based online instrument would be a strong absorbance of aerosol components absorbing at the same or similar wavelength as AA causing high background levels and poor detection limits.

To test the absorbance of ambient aerosol components, an extract from a filter collected during the Atmospheric Pollution and Human Health campaign (APHH) (Shi et al., 2019) was diluted to four concentrations that correspond to realistic outdoor air pollution levels up to  $30 \mu\text{g}/\text{m}^3$ . Filter extracts were then reacted with AA and the absorbance of AA and filter extracts was measured at 265 nm using a 1 m liquid waveguide capillary cells (LWCC, WPI) through which the extracts were pumped continuously. Unfortunately, the shoulder of the absorbance of aerosol components contributes substantially to the overall absorbance at 265 nm as can be seen in Figure S2. As the absorption properties of the aerosol could vary substantially over time, an absorbance measurement would not be a straight forward strategy to quantify the AA reactivity with an online instrument.

For offline measurements (i.e. filter extracts), the AA consumption is usually observed over time, and therefore self-absorbance is not a problem because only the relative change in the absorbance at 265nm are measured. For a true online instrument, however, measuring AA absorbance at different time points would not be feasible and therefore quantifying the AA reactivity using absorbance was not further considered in this study.

A dual channel online instrument might potentially be an option to implement AA absorbance where one channel would measure continuously the aerosol absorbance and the second channel would measure the sum of the aerosol absorbance and of AA.



1.3 **Figure S2 Absorbance of AA (black line) and ambient filter extract (blue lines) with different particle concentrations. The black line shows the absorbance of pure AA, and all the blue lines are the absorbance of filter extract without AA. The Appropriate Buffer for the AA Assay.**

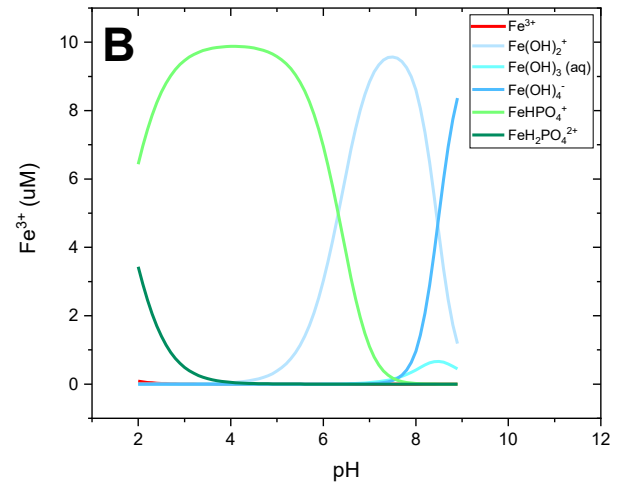
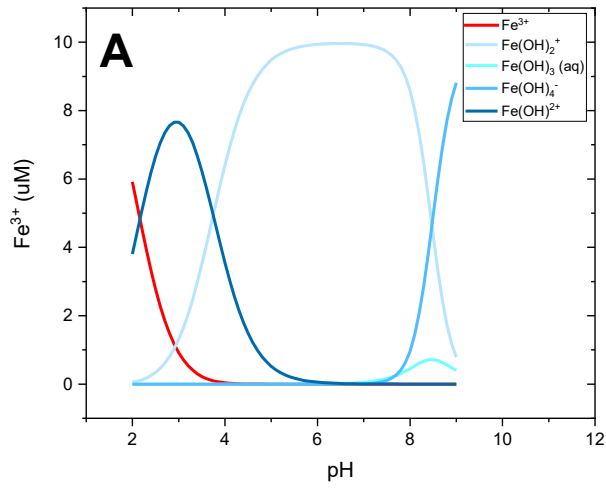
40

In many assays quantifying ROS or OP in aerosols, phosphate buffer is used (Gao et al., 2017; Pietrogrande et al., 2019; Wragg et al., 2016). Because AA reacts efficiently with metals, phosphate might severely affect OP quantification, because it may chelate metals, influencing their redox chemistry. Figure S3 illustrates the effect of phosphate buffer and HEPES buffer on soluble  $\text{Fe}^{3+}$  speciation over a pH range of 2-9 modeled with the chemical equilibrium model Visual MINTEQ. In Figure S3A the speciation of  $\text{Fe}^{3+}$  is shown when the solution is buffered with HEPES where most of the iron is present as  $(\text{Fe}(\text{OH})_2)^+$  at pH7. On the contrary, when the system is buffered with phosphate, a substantial fraction of  $\text{Fe}^{3+}$  is present as iron phosphate ( $\text{FeHPO}_4^{2+}$ ) under acidic and neutral pH conditions (Figure S3B, light green line), which might significantly affect the redox chemistry of  $\text{Fe}^{3+}$ . In the model, only species that are important for the reaction and present at a sufficient concentration are displayed.

45

50

Depending on the chosen buffer, the metal speciation can be very different. Other metals might form other complexes, but HEPES is considered to be a buffer that generally does not form strong metal complexes (Shipman, 1969; Yoshimura et al., 1992). These findings indicate that phosphate buffer is not a suitable buffer to quantify metal-initiated OP because of the chelation of phosphate with metals.



55

**Figure S3 Modeling  $\text{Fe}^{3+}$  speciation with different buffers using Visual MINTEQ. (A) HEPES buffer does not chelate metals and at pH 7 iron is almost entirely present as  $\text{Fe}(\text{OH})_2^+$ . When iron is buffered with phosphate (B), a substantial fraction of the total  $\text{Fe}^{3+}$  at pH 7 is present as iron phosphate ( $\text{FeHPO}_4^{2+}$ ).**

60 **1.4 DFQ Spectrum**

In Figure S4 a spectrum of 200  $\mu\text{M}$  DHA with 20 mM OPDA is shown. The spectrum was taken with the QePro spectrometer as described in the main text. The main peak at 430 nm is the fluorescence peak of DFQ and the small peak at 365 nm is scatter light from the LED. DFQ gets photolyzed over time to a product, which we have not characterized and which is absorbing at around 500 nm where the shoulder of a second small peak can be seen.

65 Note that this is a relative spectrum measured with the settings used in this experiment, and that the absolute peak shape could slightly change depending on the exact spectrometer type and settings.

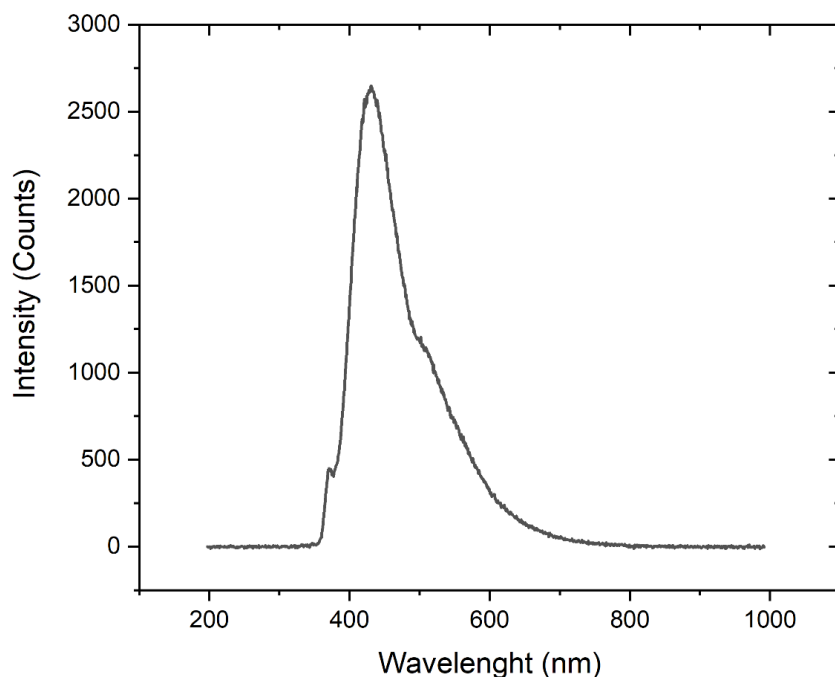


**Figure S4 DFQ Spectrum.** The small peak at 365 nm is the scattering of the LED, and the large peak at 430 nm is the emission of the DFQ. The shoulder at around 500 nm is due to an unidentified decomposition product of DFQ.

70

## References

- Campbell, S. J., Utinger, B., Lienhard, D. M., Paulson, S. E., Shen, J., Griffiths, P. T., Stell, A. C. and Kalberer, M.: Development of a physiologically relevant online chemical assay to quantify aerosol oxidative potential, *Anal. Chem.*, doi:10.1021/acs.analchem.9b03282, 2019.
- 75 Deutsch, M. J. and Weeks, C. E.: Microfluorometry Assay for Vitamin C, *J. AOAC Int.*, 48(6), 1248–1256, doi:10.1093/JAOAC/48.6.1248, 1965.
- Fang, T., Verma, V., Guo, H., King, L. E., Edgerton, E. S. and Weber, R. J.: A semi-automated system for quantifying the oxidative potential of ambient particles in aqueous extracts using the dithiothreitol (DTT) assay: Results from the Southeastern Center for Air Pollution and Epidemiology (SCAPE), *Atmos. Meas. Tech.*, 8(1), 471–482, doi:10.5194/amt-8-471-2015, 2015.
- 80 Gao, D., Fang, T., Verma, V., Zeng, L. and Weber, R. J.: A method for measuring total aerosol oxidative potential (OP) with the dithiothreitol (DTT) assay and comparisons between an urban and roadside site of water-soluble and total OP, *Atmos. Meas. Tech.*, 10(8), 2821–2835, doi:10.5194/amt-10-2821-2017, 2017.
- 85 Perrone, M. R., Bertoli, I., Romano, S., Russo, M., Rispoli, G. and Pietrogrande, M. C.: PM<sub>2.5</sub> and PM<sub>10</sub> oxidative potential at a Central Mediterranean Site: Contrasts between dithiothreitol- and ascorbic acid-measured values in relation with particle size and chemical composition, *Atmos. Environ.*, 210, 143–155, doi:10.1016/J.ATMOSENV.2019.04.047, 2019.
- Pietrogrande, M. C., Bertoli, I., Manarini, F. and Russo, M.: Ascorbate assay as a measure of oxidative potential for ambient particles: Evidence for the importance of cell-free surrogate lung fluid composition, *Atmos. Environ.*, 211(May), 103–112, doi:10.1016/j.atmosenv.2019.05.012, 2019.
- 90 Shi, Z., Vu, T., Kotthaus, S., Harrison, R. M., Grimmond, S., Yue, S., Zhu, T., Lee, J., Han, Y., Demuzere, M., Dunmore, R. E., Ren, L., Liu, D., Wang, Y., Wild, O., Allan, J., Acton, W. J., Barlow, J., Barratt, B., Beddows, D., Bloss, W. J., Calzolari, G., Carruthers, D., Carslaw, D. C., Chan, Q., Chatzidiakou, L., Chen, Y., Crilley, L., Coe, H., Dai, T., Doherty, R., Duan, F., Fu, P., Ge, B., Ge, M., Guan, D., Hamilton, J. F., He, K., Heal, M., Heard, D., Hewitt, C. N., Hollaway, M., Hu, M., Ji, D., Jiang, X., Jones, R., Kalberer, M., Kelly, F. J., Kramer, L., Langford, B., Lin, C., Lewis, A. C., Li, J., Li, W., Liu, H., Liu, J., Loh, M., Lu, K., Lucarelli, F., Mann, G., McFiggans, G., Miller, M. R., Mills, G., Monk, P., Nemitz, E., O'Connor, F., Ouyang, B., Palmer, P. I., Percival, C., Popoola, O., Reeves, C., Rickard, A. R., Shao, L., Shi, G., Spracklen, D., Stevenson, D., Sun, Y., Sun, Z., Tao, S., Tong, S., Wang, Q., Wang, W., Wang, X., Wang, X., Wang, Z., Wei, L., Whalley, L., Wu, X., Wu, Z., Xie, P., Yang, F., Zhang, Q., Zhang, Y., Zhang, Y. and Zheng, M.: Introduction to the special issue “In-depth study of air pollution sources and processes within Beijing and its surrounding region (APHH-Beijing),” *Atmos. Chem. Phys.*, 19(11), 7519–7546, doi:10.5194/acp-19-7519-2019, 2019.
- 100 Shipman, C.: Evaluation of 4-(2-hydroxyethyl)-1-piperazineethanesulfonic acid (HEPES) as a tissue culture buffer, *Proc. Soc. Exp. Biol. Med.*, 130(1), 305–310, doi:10.3181/00379727-130-33543, 1969.
- Vislisel, J. M., Schafer, F. Q. and Buettner, G. R.: A simple and sensitive assay for ascorbate using a plate reader, *Anal. Biochem.*, 365(1), 31–39, doi:10.1016/j.ab.2007.03.002, 2007.
- Wragg, F. P. H., Fuller, S. J., Freshwater, R., Green, D. C., Kelly, F. J. and Kalberer, M.: An automated online instrument to quantify aerosol-bound reactive oxygen species (ROS) for ambient measurement and health-relevant aerosol studies, *Atmos. Meas. Tech.*, 9(10), 4891–4900, doi:10.5194/amt-9-4891-2016, 2016.
- 110 Yoshimura, Y., Matsuzaki, Y., Watanabe, T., Uchiyama, K., Ohsawa, K. and Imaeda, K.: Effects of Buffer Solutions and Chelators on the Generation of Hydroxyl Radical and the Lipid Peroxidation in the Fenton Reaction

System, *J. Clin. Biochem. Nutr.*, 13, 147–154, 1992.

115 Zhang, Z.-H. H., Hartner, E., Uttinger, B., Gfeller, B., Paul, A., Sklorz, M., Czech, H., Yang, B. X., Su, X. Y.,  
Jakobi, G., Orasche, J., Schnelle-Kreis, J., Jeong, S., Gröger, T., Pardo, M., Hohaus, T., Adam, T., Kiendler-Scharr,  
A., Rudich, Y., Zimmermann, R. and Kalberer, M.: Are reactive oxygen species (ROS) a suitable metric to predict  
toxicity of carbonaceous aerosol particles?, *Atmos. Chem. Phys. Discuss.*, 22(August), 1–29, doi:10.5194/acp-  
2021-666, 2021.